Low-Temperature Magnetic Transitions in Dilute Au-Based Alloys with Cr, Mn, and Fe

O. S. LUTES AND J. L. SCHMIT
Honeywell Research Center, Hopkins, Minnesota
(Received 6 November 1963)

A study has been made of the low-temperature magnetic behavior of gold-based solid solutions containing transition metals in dilute concentration. Of particular interest are Au-Cr, Au-Mn, and Au-Fe, for which solid solutions of higher concentration have been found by other workers to undergo antiferromagnetic (Cr) and ferromagnetic (Mn and Fe) transitions. The present results show that for alloys of about 1 at.% there occur low-temperature magnetic transitions which are similar for all three solutes. The main features of the transitions, as in dilute Cu-Mn alloys, are a susceptibility maximum and, below the temperature of the maximum, a saturable remanent magnetic moment which increases with decreasing temperature in a characteristic manner. The temperature of the maximum increases nearly in proportion to concentration and also depends on the identity of the solute, being about 12, 4, and 8°K/at.%, respectively, for Cr, Mn, and Fe. In the case of Au-V and Au-Co alloys susceptibility maxima and remanent magnetization were absent.

INTRODUCTION

THE purpose of this article is to report results on the low-temperature magnetic behavior of dilute binary Au-based solid solutions containing transition metals. Because of the relatively wide solubility range in such systems they present an unusual opportunity for the study of dilution effects. Previous work on dilute Au-Cr,[1] Au-Mn,[2] and Au-Fe[3–5] alloys has demonstrated high-temperature paramagnetism, evident mainly from the Curie-Weiss law of temperature dependence of the magnetic susceptibility. The effective atomic moments deduced from this law are generally comparable in magnitude with those of the free atom. In addition, predictions from the paramagnetic Curie temperature θ_p concerning the magnetic transitions in the more concentrated alloys are fairly satisfactory. Thus Au-Cr alloys between 21.4 and 29.2 at. % Cr with large negative θ_p, exhibit antiferromagnetic transitions[6] between 274 and 383°K. Au-Mn alloys with concentrations greater than 6 at. % Mn are reported to have ferromagnetic Curie points quite close to θ_p, although some evidence of antiferromagnetism appears in the magnetization curves.[7] Similarly, Au-Fe alloys having concentrations greater than 10 or 15 at. % Fe become ferromagnetic[4,8] at temperatures fairly near θ_p. In such alloys a decrease of concentration results in a decrease of transition temperature. A continuation of this simple dilution effect to arbitrarily small concentrations has been shown unlikely, however, in the case of models based on nearest-neighbor interactions.[8,9] Such models predict cooperative transitions only for concentrations above a critical value. Theoretical estimates of the critical concentration depend upon the particular model and vary from 9 to 17 at. % for the fcc lattice.[8] Alloy concentrations in the present study were well below these levels. The available temperature range also extended below transition temperatures to be expected on the basis of simple dilution.

TABLE I. Solute resistivities.

Alloy	Concentration (at. %)	T(°K)	ρ (μohm-cm/at. %) Present work	Literature values	
Au-V	1.0	300	14.4	14.0[a]	
Au-Cr	0.5	300	5.1	4.25[a]	
Au-Cr	1.0	300	4.2	4.25[a]	
Au-Mn	1.0	300	2.37	2.41[a]	2.23[b]
Au-Mn	2.0	300	2.24	2.41[a]	2.23[b]
Au-Fe	0.5	300	8.1	7.9[a]	8.0[b]
Au-Fe	1.0	300	8.1	7.9	7.9[b]
Au-Co	1.0	4	5.9	5.9[c]	

[a] J. O. Linde, Physica **24**, 5109 (1958). Limiting values as concentration approaches zero.
[b] C. A. Domenicali and E. L. Christenson, Ref. 10. Values for Au-Mn are for 10 at.%Mn. Values for Au-Fe are obtained from interpolation, using author's data.
[c] A. N. Gerritsen, Physica **25**, 489 (1959).

EXPERIMENTAL PROCEDURE

Alloys were made with the following nominal concentrations (atomic percent): 1% V, 0.5% Cr, 1% Cr, 1% Mn, 2% Mn, 0.5% Fe, 1% Fe, 1% Co. The alloys were made by melting about 35 g of mint gold (Baker Platinum Division, Englehard Industries[10]) together with the required weight of solute (obtained from Johnson-Matthey) in a sealed, evacuated 7-mm internal-diameter quartz tube at 1200°C. After agitating and holding in the molten state for about 20 h, the

[1] A. Giansoldati, Arkiv Fysik **8**, 151 (1954).
[2] G. Gustafsson, Ann. Physik **25**, 545 (1936).
[3] J. W. Shih, Phys. Rev. **38**, 2051 (1931).
[4] A. R. Kaufmann, S. T. Pan, and J. R. Clark, Rev. Mod. Phys. **17**, 87 (1945).
[5] E. Scheil, H. Specht, and E. Wachtel, Z. Metallkunde **49**, 590 (1958).
[6] E. Wachtel and V. Vetter, Z. Metallkunde **52**, 525 (1961).
[7] J. Cohen, G. Quezel, and G. Rimet, *Berichte der Arbeitsgemeinschaft Ferromagnetismus 1959* (Verlag Stahleisen M. B. H., Dusseldorf, 1960), p. 74.
[8] H. Sato, A. Arrott, and R. Kikuchi, Phys. Chem. Solids **10**, 19 (1959).
[9] J. S. Smart, Phys. Chem. Solids **16**, 169 (1960).
[10] C. A. Domenicali and E. L. Christenson, J. Appl. Phys. **32**, 2450 (1961).

TABLE II. Magnetic isotherms.

Alloy	T (°K)	H (Oe)	10^2M (emu/g)
0.5% Cr	1.31	960	0.32
		2090	0.69
		2940	1.04
		3880	1.49
		4880	1.78
		5850	2.18
1% Cr	1.30	250	0.13
		1000	0.35
		2000	0.71
	1.32	2030	0.70
		3420	1.16
	1.98	2030	0.70
		3420	1.19
1% Mn	0.52	200	0.66
		400	1.36
	1.30	207	0.82
		410	1.66
	2.03	205	0.89
		396	1.83
	2.53	205	0.97
		412	1.93
	3.03	205	1.03
		407	2.08
	3.52	205	1.09
		405	2.16
	4.06	197	1.04
		391	2.16
	4.57	197	1.11
		380	2.12
	5.02	193	1.08
		370	2.05
	10.0	208	0.51
		396	0.97
		824	1.98
2% Mn	1.28	100	0.52
		213	1.14
		300	1.65
		400	2.20
		600	3.34
		800	4.58
		1000	5.88
0.5% Fe	1.30	950	0.37
		2080	0.84
		2900	1.23
		3850	1.66
	4.18	956	4.62
		2100	1.02
		2940	1.39
1% Fe	1.29	212	0.10
		400	0.17
		800	0.39
		998	0.49
		1195	0.58
	4.19	209	0.12
		400	0.23
		600	0.36
		800	0.49
		1000	0.61
		1200	0.79
		1420	0.92
		1620	1.08
1% V	1.31	1000	0.053
		5000	0.245

temperature was lowered to 1000°C, where homogenization was carried out for 6 h. The alloy was then quenched in water. A section of the resulting ingot was formed into a $\frac{1}{4}$-in.-diam sphere by pressing and filing. The sphere was carefully cleaned and etched before mounting. Samples for resistivity measurements were taken from regions of the ingot adjacent to that used for the sphere. These samples were rolled and drawn into wire, then annealed for 5 h at 500°C. The resistivity measurements were carried out mainly at room temperature, and were for the purpose of insuring that the solute was actually in solution. For this purpose the solute resistivity was calculated by subtracting from the total resistivity the resistivity of the gold, measured separately. The agreement with literature values of solute resistivity was then used as the criterion for validity of the nominal alloy concentrations. The resistivity results are shown in Table I. The agreement is regarded as satisfactory with the possible exception of the 0.5% Cr alloy.

Susceptibility and remanent moment measurements were carried out in the 0.5–35°K range with magnetic fields available from 0 to 13 kOe, using apparatus described previously.[11] In order to evaluate any contributions from sources other than the solute, a run was carried out using a pure gold sphere in the sample holder. The combination of gold sphere and sample holder showed no measurable remanence and required a susceptibility correction which was usually negligible in the temperature range of the measurements.

The apparatus was calibrated for absolute values of magnetic moment by means of magnetization measurements on a superconducting lead (Pb) sphere of accurately measured volume, assuming the ideal volume susceptibility, $(-3/8\pi)$. The limit of detectability of the apparatus expressed in total moment was about 10^{-4} emu of magnetic moment, expressed in specific moment about 4×10^{-5} emu/g, and expressed in susceptibility at maximum field about 4×10^{-9} emu/g.

RESULTS AND DISCUSSION

Magnetic Susceptibility

Magnetic susceptibilities were determined by evaluation of the initial slopes of the magnetization isotherms. This evaluation could be made by measurements at a single field, provided the field was sufficiently small. In order to choose the fields for susceptibility measurements a survey of magnetic isotherms for all the alloys,

[11] O. S. Lutes and J. L. Schmit, Phys. Rev. **125**, 433 (1962).

TABLE III. Susceptibility data.

	T (°K)	$10^6\chi$ (emu/g)		T (°K)	$10^6\chi$ (emu/g)		T (°K)	$10^6\chi$ (emu/g)		T (°K)	$10^6\chi$ (emu/g)
0.5% Cr	0.57	2.91	1% Cr	11.1	4.83	2% Mn	11.4	62.2	0.5% Fe	24.0	1.46
(2000 Oe)[a]	1.38	3.53	(3420 Oe)	12.8	4.82	(500 Oe)	13.6	51.2	(2000 Oe)	25.1	1.49
	2.47	3.85		13.8	4.92		15.6	43.4		26.5	1.42
	3.30	4.04		14.9	4.79		17.5	37.9		28.6	1.34
	4.7	4.40		15.8	4.75		20.0	32.3		29.9	1.27
	4.8	4.55		17.5	4.63		25.2	24.2			
	5.3	4.44		19.4	4.19		28.5	21.4	1% Fe	0.54	4.40
	5.7	4.40		22.5	3.83		32.9	18.4	(1000 Oe	1.35	4.78
	6.3	4.52		26.5	3.03		35.3	18.1		2.06	4.94
	6.9	4.37					36.9	17.1		3.20	6.06
	7.7	4.42								4.18	6.48
	8.7	4.31	1% Mn	0.52	33.7	0.5% Fe	1.30	4.11		5.0	7.08
	9.7	4.05	(500 Oe)	1.30	40.2	(2000 Oe)	2.29	4.58		6.0	7.33
	10.6	3.85		2.03	44.8		3.31	4.88		6.8	7.62
	11.5	3.72		2.53	47.3		3.50	4.86		8.6	7.46
	12.4	3.56		3.03	50.9		3.67	4.91		7.4	7.53
	13.3	3.40		3.50	52.9		3.82	4.82		7.9	7.43
	14.3	3.08		3.82	53.8		4.00	4.75		8.6	7.40
	15.4	2.99		4.19	54.5		4.31	4.82		9.6	6.98
	16.3	2.77		4.5	54.5		5.0	4.69		11.5	6.12
	17.0	2.64		4.9	53.0		6.1	4.64		14.1	5.26
	17.9	2.51		5.6	47.0		7.0	4.16		16.1	4.59
	18.9	2.45		6.2	43.1		7.9	3.85		18.2	3.86
	19.6	2.37		8.3	30.2		8.9	3.46		21.5	3.32
	20.6	2.29		10.0	24.1		9.9	3.15		26.2	2.68
	21.7	2.11		13.8	17.1		10.7	3.07			
	22.0	2.07		18.2	12.4		11.7	2.83	1% Co	0.52	2.17
	25.1	1.86		24.1	8.6		12.6	2.72	(1000 Oe)	0.70	1.88
	27.2	1.70		33.5	6.5		13.7	2.46		1.29	1.55
	29.6	1.67					14.7	2.37		3.0	1.17
			2% Mn	1.28	55.8		15.2	2.30		6.0	0.78
1% Cr	1.32	3.39	(300 Oe)	4.18	77.8		15.7	2.11		10.0	0.71
(3420 Oe)	1.98	3.51		4.38	80.4		16.3	2.19	1% V	0.52	0.66
	2.60	3.72		4.95	85.0		16.5	2.00	(5000 Oe)	1.31	0.49
	4.04	4.03		5.9	91.6		16.9	2.11		2.1	0.47
	5.15	4.27		6.6	93.6		17.6	1.96		3.0	0.42
	6.2	4.39		6.8	93.1		18.8	1.91		4.0	0.40
	7.4	4.49		7.4	93.4		19.6	1.91		5.0	0.38
	8.4	4.75		7.9	91.6		20.1	1.80		6.0	0.38
	9.4	4.83		8.6	85.6		21.4	1.73		8.0	0.35
	10.6	4.88		9.6	76.6		23.1	1.54		10.0	0.35

[a] Field in which χ determined.

except 1% Co, was made at selected temperatures. The data are tabulated in Table II. Susceptibility versus temperature curves are plotted in Fig. 1, and the complete data tabulated in Table III. The alloys of Cr, Mn, and Fe exhibit susceptibility maxima at temperatures which depend upon the identity and concentration of the solute. The V and Co susceptibilities show a monotonic decrease with increasing temperature. The occurrence of susceptibility maxima in dilute alloys of this general class has previously been established only in the case of Mn as solute and with solvents other than Au. Further discussion concerning the susceptibility maxima is to be found in a later section.

In view of the known high-temperature paramagnetic behavior in the case of Cr, Mn, and Fe, it is of interest to compare the temperature dependence above the susceptibility maxima with the Curie-Weiss law

$$\chi = N\mu^2/3k(T-\theta_p), \qquad (1)$$

where N is the number of atoms, μ the effective moment per atom, k the Boltzmann constant, and θ_p the paramagnetic Curie temperature. The comparison is made in Fig. 2 by plotting χ^{-1} versus T for all alloys. The V and Co data do not fall on straight lines over any substantial portions of the temperature range. For the other alloys the effective moment p_{eff} in Bohr magnetons per atom of dissolved element is calculated from the expression

$$p_{\text{eff}} = (3k)^{1/2}/\mu_B[A\,(d/dT)\chi_{\text{mol}}^{-1}]^{1/2}, \qquad (2)$$

where χ_{mol} is the susceptibility per mole of solute, A is Avogadro's number, and μ_B the Bohr magneton. Table IV shows p_{eff} and θ_p taken from the data of Fig. 2, together with literature values for dilute concentrations. The temperature range from which each value is determined is also given. In the case of θ_p, determined from the intercept on the T axis, high-temperature determinations are quite sensitive to change of slope. Consequently even a slight curvature in the high-temperature χ^{-1} plots can explain what appear to be

TABLE IV. Paramagnetic properties.

Alloy	Concentration (at. %)	Source	Temperature range used (°K)	p_{eff}	θ_p (°K)
Au-Cr	0.5%	Present work	10–30	4.0	−2
	1.0	Present work	15–30	3.7	−3
	0 to 10	Wachtel and Vetter[a]	150–1000	4.1[b]	(0 to −100)[b]
	0 to 10	Giansoldati	300–500	4.9[b]	0 to −300
Au-Mn	1.0	Present work	6–34	5.8	1.5
	2.0	Present work	8–37	6.6	2.9
	1.8	Cohen *et al.*	4–400	5.6	15[c]
	0.72	Gustafsson	300–700	5.5	...
	2.08	Gustafsson	300–700	5.8	...
Au-Fe	0.5	Present work	6–30	3.6	−3
	1.0	Present work	10–25	3.3	1
	0.63	Kaufmann *et al.*	14–77	3.0	−2[c]
	0.63	Kaufmann *et al.*	77–300	3.4	−25[c]
	0 to 10	Scheil *et al.*	100–1200	(4.9 to 4.8)[b]	(−30 to 100)[b]

[a] Journal references may be found in text. [b] From author's smoothed curves. [c] Estimated using author's data.

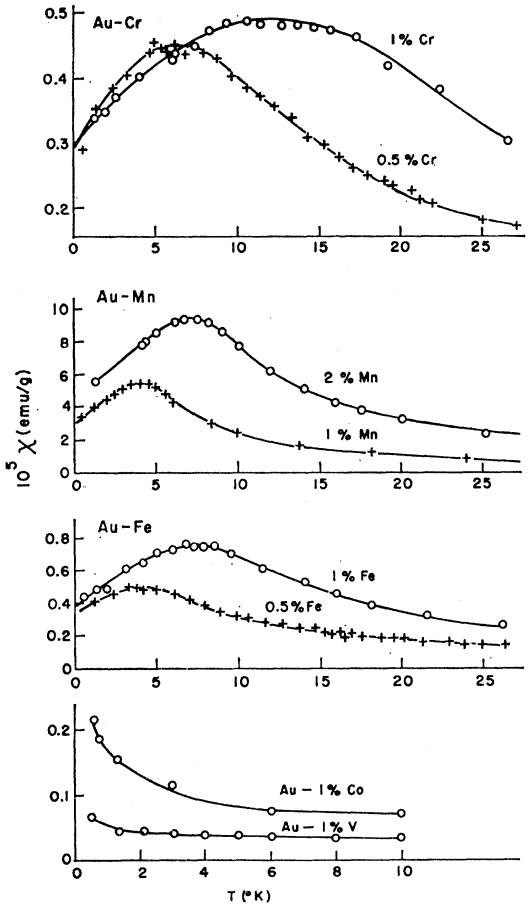

FIG. 1. Magnetic susceptibility versus temperature. χ is the susceptibility per gram of alloy.

large differences in θ_p.[12] The value of p_{eff} for 2% Mn also warrants comment, since the largest expected value would be 5.9, based on a spin of $\frac{5}{2}$ (see below). That this discrepancy occurs in the alloy of highest concentration is probably significant. A property of theoretical models treating the susceptibility maxima in dilute Cu-Mn alloys[13] is the increasing breadth of the maximum with increasing solute concentration. This corresponds to increasing departure from linearity of χ^{-1} with increasing solute concentration for temperatures immediately above the temperature of the maximum. This effect would be in the direction to give

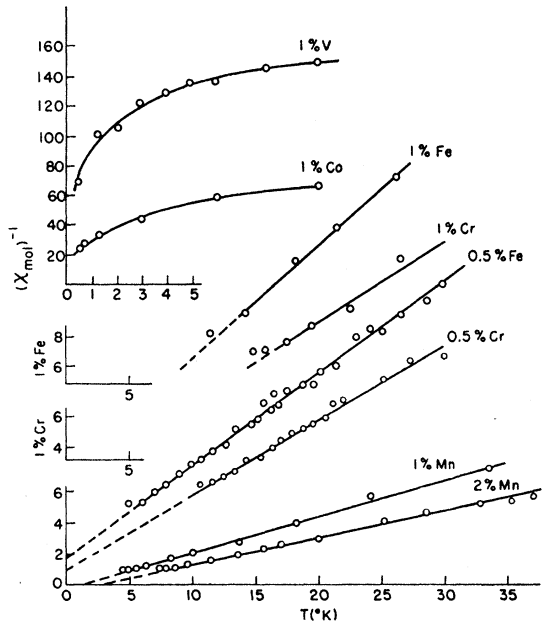

FIG. 2. Curie-Weiss law. χ_{mol} is the susceptibility in emu per mole of solute, and is given by the expression $\chi_{\text{mol}}=\chi(\text{emu/g}) \times W/C$, where W is the atomic weight of the alloy and C the atomic fraction of solute. For those alloys showing linear dependence the magnitude of the slope is inversely proportional to the square of the effective moment per atom.

[12] Note particularly that choice of temperature range in the Kaufmann *et al.* data affects θ_p more than p_{eff}. The discrepancy in θ_p in the case of the Cohen *et al.* data is very likely also not real since the latter data apparently included low-temperature points only at 4.2 and 20.4°K.

[13] A. J. Dekker, Physica **24**, 697 (1958).

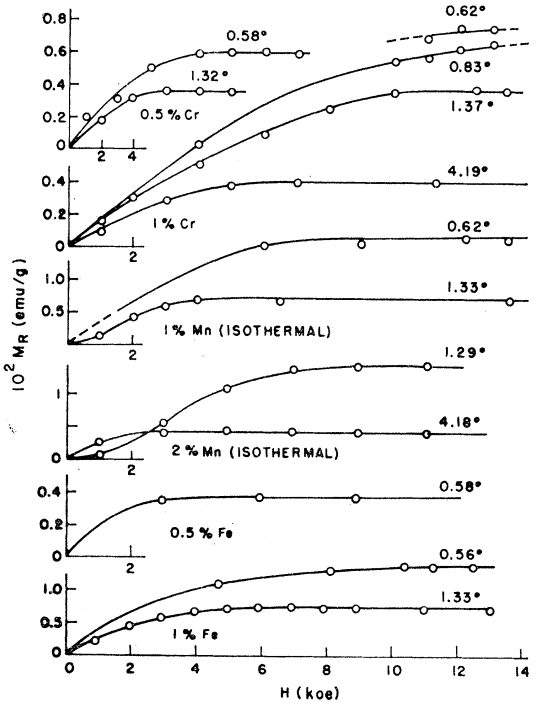

FIG. 3. Field saturation of remanence. M_R is the remanent moment per gram of alloy. For the Mn alloys the saturation was carried out isothermally. The other alloys were field cooled.

erroneously high p_{eff} at higher concentrations when p_{eff} is obtained from the best straight line on a χ^{-1} plot. Aside from the 2% Mn alloy our p_{eff} values are seen to agree fairly well with the high-temperature determinations.

In the theory of paramagnetism p_{eff} is related to the angular-momentum quantum number J of the constituent moments by

$$p_{\text{eff}}=g[J(J+1)]^{1/2}, \tag{3}$$

where g is the gyromagnetic ratio. If J is composed of spin only, so that $J=S$ and $g=2$, Eq. (3) reduces to

$$p_{\text{eff}}=2[S(S+1)]^{1/2}. \tag{4}$$

With Eq. (4), our p_{eff} results give S equal to about $\frac{3}{2}$ for Cr, $\frac{5}{2}$ for Mn, and somewhat less than $\frac{3}{2}$ for Fe.

The paramagnetism observed in the Cr, Mn, and Fe alloys and its absence in the V alloy are in general agreement with high-temperature measurement.[14] Au-Co alloys, however, have been reported to show paramagnetic behavior at high temperature.[15] Recent theoretical views[16] predict that paramagnetism in dilute alloys is favorable if the impurity d shell is not too empty or too full. In light of these considerations and the results shown in Figs. 1 and 2 it seems likely that the Co alloy is marginal in behavior.

Magnetic Remanence

A remanent magnetic moment was found in the Cr, Mn, and Fe alloys at temperatures below the susceptibility maxima after applying a field. This moment could be field-saturated by increasing the field at constant temperature (isothermal saturation) or by field cooling, as observed for Cu-Mn alloys.[17,11] In the field-cooling method, the alloy is cooled in successively larger fields to the nominal temperature from a starting temperature at which the remanence is saturated. Saturation curves are shown in Fig. 3 for all alloys. The field required for isothermal saturation H_I increased at lower temperatures and at higher concentrations. This is apparent from the Mn data of Fig. 3. Time decay of the remanent moment was observed near the temperature of the susceptibility maximum. The time constant was always large compared with the time of measurement.

Figures 4 and 5 show the temperature dependence of the field-saturated remanence M_{RS} for all six alloys. In each case the intercept on the temperature axis $T_c(M_{RS})$ is quite close to the temperature of the susceptibility maximum $T_c(\chi)$ determined from Fig. 1. The presence of a field-saturable remanent moment is therefore a characteristic property of the magnetic state of these alloys below the transition temperature. It is of interest to estimate the limiting value of the remanence at 0°K, M_{RSO}. It is not immediately evident, from plots such as those of Figs. 4 and 5, whether M_{RS}

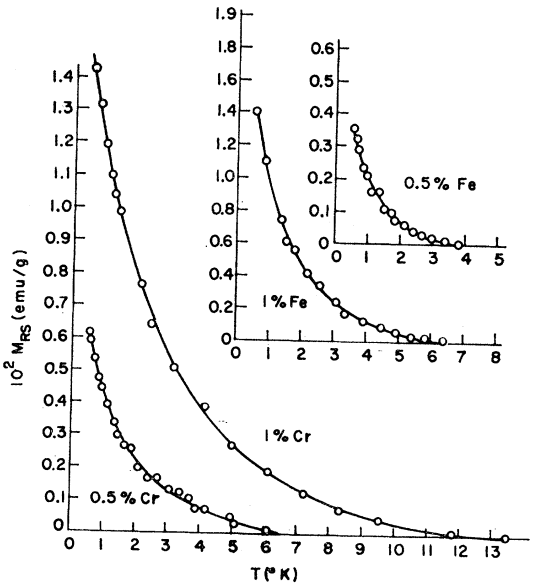

FIG. 4. Temperature dependence of saturated remanence, Au-Cr and Au-Fe alloys.

[14] E. Vogt, Z. Metallkunde **27**, 40 (1935); E. Vogt and D. Gerstenberg, Ann. Physik **4**, 145 (1959).
[15] E. Hildebrand, Ann. Physik **30**, 593 (1937).
[16] J. Friedel, Can. J. Phys. **34**, 1190 (1956); A. Blandin and J. Friedel, J. Phys. Radium **20**, 160 (1959).
[17] I. S. Jacobs and R. W. Schmitt, Phys. Rev. **113**, 459 (1959).

continues to increase indefinitely to the saturation moment of the solute, or saturates at a lower value. The most useful alloy for the purpose of extrapolation is Au-1%Cr, since it has the highest T_c and therefore the most extensive data at low temperatures. Figure 6 shows the data for this alloy on a $1/T$ basis in the lower temperature region. M_{RS} was obtained at the two lowest temperatures by a short extrapolation of the field-saturation data (see Fig. 3) using the expression $M_{RS}-M_R=\text{const}/H^2$, which generally approximates the field-cooling data. Also shown in Fig. 6 are several two-parameter expressions describing magnetic saturation as $T\rightarrow 0$. In each expression the parameters M_{RSO} and a are used to insure agreement with the data at 4.10°K ($1/T=0.243$) and at the lowest temperature, 0.605°K ($1/T=1.66$). It is evident that the well-known $\frac{3}{2}$ power law for temperature saturation of the spontaneous moment in ferromagnetic materials does not apply here and, more generally, the expression $M_{RSO}(1-aT^{\alpha})$ is inadequate for *any* choice of α. A much better approximation to the limiting form of temperature dependence, and therefore a better means of extrapolation, is given by the expression for paramagnetic saturation, $M_{RSO}B_{3/2}(a/T)$, where $B_{3/2}$ is the Brillouin function for angular-momentum quantum number $\frac{3}{2}$, and a is a constant which is equivalent to a constant magnetic field. The M_{RSO} given by this expression[18] may be compared with the saturation moment of the solute, $cAgJ\mu_B/W$ per gram, where c is the atomic fraction of Cr atoms, g the gyromagnetic ratio, J the effective quantum number per Cr atom, and W the atomic weight of the alloy. If $g=2$ and $J=\frac{3}{2}$,

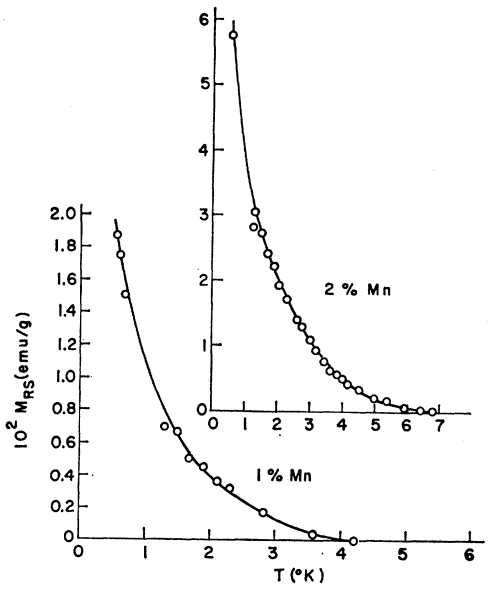

FIG. 5. Temperature dependence of saturated remanence, Au-Mn alloys.

[18] Use of Brillouin functions of higher index does not change the result greatly, the extreme case B_∞ (the Langevin function) giving only a 15% increase in the estimate of M_{RSO}.

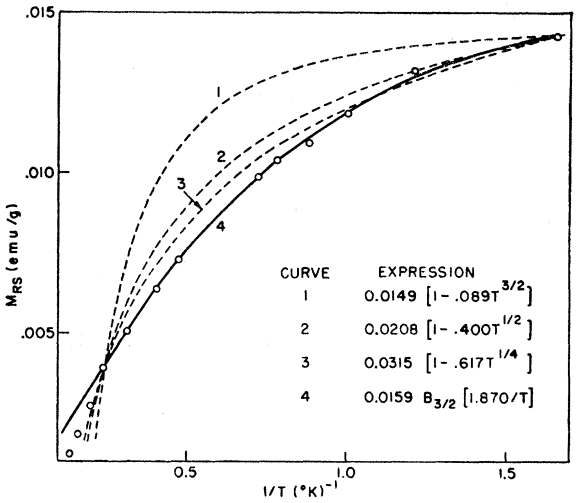

FIG. 6. Temperature-saturation of remanence. This graph shows the low-temperature remanence data for Au-1% Cr plotted against $1/T$. Several two-parameter expressions are compared with the data and with each other over the range $1/T=0.243$ to $1/T=1.66$ by adjusting them to agree with the data at the extremes of the range.

consistent with p_{eff} from our susceptibility measurements, the value for M_{RSO}, 0.0159 emu/g, is found to be 1.8% of the saturation moment (1.8% alignment). Regarding the other alloys the paramagnetic expression applies to a smaller range and is correspondingly less well defined. Estimates of alignment are a few percent in each case. Finally we note that the paramagnetic expression with constant field cannot apply to data near T_c, since it predicts zero remanence only at infinite temperature. As a low-temperature approximation, however, it applies to the 1% Cr data over nearly a decade of temperature at the low end of the available temperature range.

To summarize the above analysis, the limiting temperature dependence as $T\rightarrow 0$ of the saturated magnetic remanence of Au-1% Cr is given by the law for paramagnetic saturation to significantly better accuracy than by other two-parameter expressions which have been examined. Our best resulting estimate of the limiting remanent moment of this alloy at 0°K is about 2% of the possible Cr moment.

Discussion of the Magnetic Transition

A summary of the magnetic transition temperatures is given in Table V. It may be seen that T_c is roughly proportional to concentration but varies widely between alloys, being about 4°K/at.% Mn, 8°K/at.% Fe, and 12°K/at.% Cr. The magnetic transitions described here may be discussed in relation to those found by other workers at high concentrations of the same alloy. Figure 7 is one form of comparison. The data at higher concentrations are the ferromagnetic Curie temperatures[4,7] for Fe and Mn, and the Néel temperatures[6] for Cr. For each alloy the two lowest concentration points

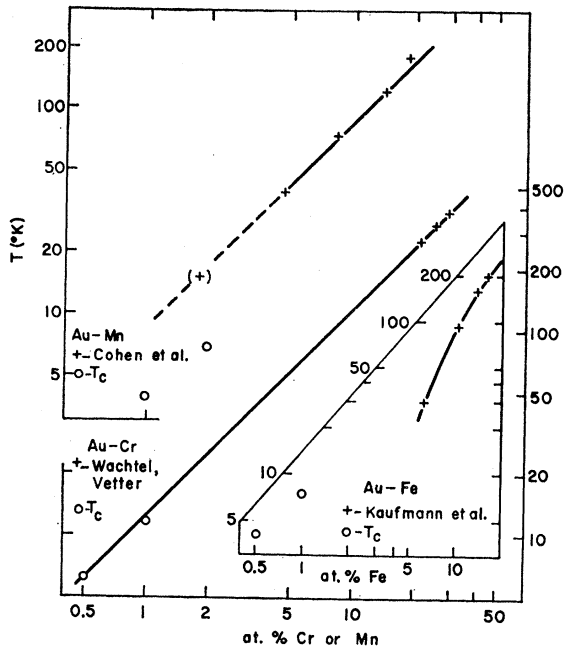

FIG. 7. Magnetic-transition temperature versus concentration. For Fe and Mn+ denotes ferromagnetic Curie temperature as determined by the authors listed. (+) is the *paramagnetic* Curie temperature at the given concentration, taken from the authors' graph. For Cr, + denotes Néel temperature determined by Wachtel and Vetter. o symbols are T_c determined by present investigation.

give T_c from the present investigation. It may be concluded that the transition temperatures for Mn and Fe are not obtainable by simple extrapolation from the Curie temperatures of the more concentrated alloys. For the Au-Cr alloys, however, extrapolation from the Néel temperatures of the concentrated alloys gives values in approximate agreement with our results.[19] In general the results suggest that all three dilute systems undergo the same kind of low-temperature magnetic transition regardless of their various magnetic behaviors at higher concentrations. It appears that although the limiting form of the magnetic state approached by Au-Mn and Au-Fe at high concentrations is ferromagnetism, another distinct form is approached at low concentrations and is characterized by a susceptibility maximum and by remanence behavior of the type reported here. The high- and low-concentration results serve, therefore, to bracket a range of concentration in which the form of the magnetic behavior of Au-Mn and Au-Fe undergoes a change. In the Au-Cr alloys the susceptibility maxima represent a less drastic change from the classical antiferromagnetic transitions observed by Wachtel and Vetter at higher concentrations.

TABLE V. Magnetic transition temperatures.

Alloy	$T_c(\chi)$ (°K)	$T_c(M_{RS})$ (°K)
0.5% Cr	6.3	6.6
1.0% Cr	11.5	11.9
1.0% Mn	4.2	4.0
2.0% Mn	7.0	6.5
0.5% Fe	4.0	4.0
1.0% Fe	7.4	6.5

[19] In the data of Wachtel and Vetter the antiferromagnetic transition was not observed for alloys of 12.6 and 7.5 at.%. According to Fig. 7 the 12.6 at. % alloy would have its transition at about 160°K, which appears to be very close to the lowest temperature used by the above mentioned investigators.

The properties of the magnetic transitions reported here are similar to those investigated extensively in dilute Cu-Mn alloys.[20,11] A susceptibility maximum has also been observed in a Ag 4 at.% Mn alloy,[20] and probably exists in dilute Mg-Mn alloys.[21] Both susceptibility maxima and magnetic hysteresis have been studied in somewhat more concentrated Cu-Mn and Ag-Mn alloys.[22] The magnetic phenomena in Cu-Mn are usually associated with a low-temperature resistance anomaly. This anomaly was first discovered by Gerritsen and Linde in Ag-Mn and subsequently established with various degrees of certainty in dilute Cu-Mn, Au-Mn, Au-Fe, and Au-Cr alloys.[23] The anomaly, which has been most firmly established for Cu-Mn,[24] consists of a resistivity minimum followed by a maximum at a lower temperature, T_{max}. It is the maximum which is apparently peculiar to transition-metal solutes.[23] An examination of the Cu-Mn literature[11,20,24] indicates that for comparable nominal concentrations T_{max} is greater than T_c. In view of the present results a similar comparison is of interest for the Au-based alloys. Such a comparison is made uncertain, however, by lack of resistivity data in the 4–14°K range, making it necessary to estimate T_{max} by extrapolation in temperature. There is a general lack of agreement between T_{max} and T_c, with T_{max} usually higher and less concentration-dependent than T_c.

SUMMARY

Dilute binary Au-based solid solutions containing Cr, Mn, or Fe in concentrations of about 1 at.%, exhibit low-temperature susceptibility maxima at temperatures approximately proportional to the alloy concentration. Above the maxima, these alloys exhibit temperature-dependent paramagnetism with effective magneton numbers generally consistent with high-temperature behavior. Below the maxima, remanent magnetization is observed. These characteristics are quite similar to those previously found in Cu-Mn alloys.

[20] J. Owen, M. E. Browne, V. Arp, and A. F. Kip, Phys. Chem. Solids **2**, 85 (1957).
[21] E. W. Collings and F. T. Hedgcock, Phys. Rev. **126**, 1654 (1962).
[22] J. S. Kouvel, Phys. Chem. Solids **21**, 57 (1961); **24**, 795 (1963).
[23] A. N. Gerritsen and J. O. Linde, Physica **17**, 573 (1951); **18**, 877 (1952); A. N. Gerritsen, *ibid.* **19**, 61 (1953); **23**, 1087 (1957).
[24] R. W. Schmitt and I. S. Jacobs, Phys. Chem. Solids **3**, 324 (1957).

Estimates of the saturated magnetic remanence at 0°K were obtained by fitting the low-temperature remanence data to paramagnetic expressions. The resulting estimates corresponded to a few percent of the available total moment of the solute atoms.

The magnetic transitions did not occur in Co and V alloys of 1 at.% concentration. These alloys also did not exhibit a Curie-Weiss law. The occurrence of the transition in the case of Cr, Mn, and Fe does not follow uniquely from the particular form of magnetic transition exhibited at higher concentrations. Instead the properties of the transition appear to be a general consequence of dilution in those alloys for which the transition-metal impurities exhibit strong paramagnetism.

ACKNOWLEDGMENTS

These experiments were carried out in the Solid State Physics Section and cooperation of various members of that group is greatly appreciated. We wish to acknowledge in particular the assistance of D. A. Clayton in some of the measurements.

PHYSICAL REVIEW VOLUME 134, NUMBER 3A 4 MAY 1964

Nonlinear Optical Theory in Solids

HUNG CHENG* AND P. B. MILLER
IBM Watson Research Center, Yorktown Heights, New York
(Received 16 December 1963)

We use a simple rule giving the expectation value of a quantum operator for any perturbation order to calculate the general second-order conductivity tensor of a solid. The expression for the conductivity tensor amounts to a regrouping of terms in the conventional expressions and takes a considerably simplified form. The formula is applied to second harmonic generation in a free-electron gas and reduces to the classical equation given by Kronig and Boukema in the optical region. The second harmonic radiation generated in metals is shown to possess two resonances occuring at the plasma oscillation frequency for p polarization and at half the plasma frequency for p and s polarization. The amplitude of the resonance is related to the imaginary part of the dielectric constant at the plasma frequency, $\epsilon_2(\omega_p)$. Only metals with $\epsilon_2(\omega_p)\ll 1$ (i.e., alkali metals, Ag and Al) will show resonant effects.

1. INTRODUCTION

THE quantum-mechanical treatment of second harmonic generation has been considered by many authors.[1,2] As the conventional calculation for the second-order conductivity involves much algebraic complexity, and the expression obtained contains many terms, the formula has been studied in detail only in the dipole approximation.

Instead of following the conventional procedure, we make use of a rule which gives the expectation value of a quantum operator for any perturbation order.[3] Our expression for the conductivity tensor amounts to a regrouping of terms in the conventional expression and takes a simplified form.[3a] We next apply this formula to the study of second harmonic generation in a free-electron gas and find that in the optical region, the second-order conductivity tensor agrees with the classical form,[4] which is of the same order of magnitude as the experimentally observed second-order conductivity tensor of some solids like KDP, which lack inversion symmetry. The second harmonic radiation generated in metals is shown to possess two resonances, occurring at the plasma oscillation frequency and half the plasma oscillation frequency which arise from the resonance of the plasma oscillation with the fundamental and the second harmonic radiation, respectively. These resonance effects further enhance the possibility of large second harmonic production in metals.

2. THE CONDUCTIVITY TENSOR

Let us consider the interaction of an electromagnetic field with a system which is originally described by a Hamiltonian H_0. In a solid H_0 will be the kinetic energy plus a periodic potential. The interaction Hamiltonian is

$$H'=-\frac{e}{2mc}[\mathbf{A}(x,t)\cdot\mathbf{p}+\mathbf{p}\cdot\mathbf{A}(x,t)]+\frac{e^2}{2mc^2}A^2(x,t), \quad (1)$$

where $\mathbf{A}(x,t)$ is the vector potential for the electromagnetic field, the gauge being chosen so that the scalar potential is zero and $\mathbf{p}=-ih\nabla$. Denoting C_s^+ and C_s as the electron creation and annihilation operator of state s, which is an eigenstate of the unperturbed Hamiltonian

* Present address: Department of Physics, Princeton University, Princeton, New Jersey.

[1] J. A. Armstrong, N. Bloembergen, J. Ducuing, and P. S. Pershan, Phys. Rev. **127**, 1918 (1962).

[2] P. N. Butcher and T. P. McLean, Proc. Phys. Soc. (London) **81**, 219 (1962).

[3] Hung Cheng (to be published).

[3a] *Note added in proof.* A similar formalism has also been used by P. L. Kelley, Phys. Chem. Solids **24**, 607 (1963); **24**, 1113 (1963).

[4] R. Kronig and J. I. Boukema, Koninkl. Ned. Akad. Wetenschap. Proc. Ser. B **66**, 8 (1963).